Journal of Molecular Liquids 383 (2023) 122120

Contents lists available at ScienceDirect

Journal of Molecular Liquids

journal homepage: www.elsevier.com/locate/molliq

# Choline chloride-water mixtures as new generation of green solvents: A comprehensive physico-chemical study

Emanuela Mangiacapre [a], Franca Castiglione [b], Matteo D'Aristotile [a], Valerio Di Lisio [c], Alessandro Triolo [d,*], Olga Russina [a,d,*]

[a] Department of Chemistry, University of Rome Sapienza, Rome 00185, Italy
[b] Department of Chemistry, Materials and Chemical Engineering "Giulio Natta", Politecnico di Milano, 20133 Milan, Italy
[c] Donostia International Physics Center, Paseo Manuel Lardizabal 4, 20018 Donostia/San Sebastian, Spain
[d] Laboratorio Liquidi Ionici, Istituto Struttura della Materia, Consiglio Nazionale delle Ricerche (ISM-CNR), Rome 00133, Italy

ARTICLE INFO

*Keywords:*
Hydrogen bonding
Hydrophilic
Sustainable
Choline chloride
Melting point

ABSTRACT

Natural deep eutectic solvents (NADES) are an increasingly appreciated class of mixtures composed by eco-sustainable and environmentally responsible components with hydrogen bonding (HB) donor and acceptor capabilities that enable the establishment of an extended HB network. The latter eventually leads to a substantial drop in the mixture melting point with respect to the one of the ideal mixture. Water-based NADES represent an exciting system that responds to the above mentioned criteria and contain water as a major component, rather than as an impurity or a deliberately added minor ingredient. Choline Chloride (ChCl, a well known HB acceptor in DES systems) forms NADES when mixed with water, which plays the role of HB donor. Several applications have already been identified for this system, but chemical physical properties of choline-rich mixtures, including the DES concentration, are not well established, yet. In order to overcame this limitation and introduce a subsequent, more systematic investigation of atomistic organization in these mixtures, here we report results from a series of chemical physical characterizations of water:ChCl with ratio ranging from 2 to 10 between ca. 280 and 330 K. Calorimetric measurements, density, viscosity, electric conductivity, refractive index, X-ray diffraction patterns and several $^{1}H$ and $^{35}Cl$ NMR spectroscopy observables are reported and compared with literature (when available). The deep eutectic nature of the water: ChCl 4:1 mixture is assessed, leading to the individuation of *aquoline*, as the corresponding DES. The other chemical physical properties are observed to vary, upon water content, in a monotone way, without abrupt changes across the eutectic concentration, thus providing support for the exploitation of the ChCl/water class of solvents, with tunable chemical-physical properties across their wide liquid range.

## 1. Introduction

Choline (Ch, 2-hydroxyethyl-trimethylammonium, vitamin B4) Chloride (ChCl) is a nutritional additive and a safe supplement to animal food. It is a safe, non-toxic, biodegradable and easily accessible ionic compound, with melting point ca. 300 °C. It is one of the most well-known and used components for formulation of natural deep eutectic solvents (NADES) [1-6], a recently proposed class of mixtures, which are composed by naturally occurring and sustainable components and show a melting point below the one expected from the ideal behaviour of the mixture. These media are presently attracting great attention as an environmentally sustainable class of materials addressing several societal calls [2-4,7,8]. Among the existing classes of DES, Type III DES [9] are typically prepared by mixing ionic compounds (generally developing extended hydrogen bonding mediated networks), such as ChCl, with hydrogen bonding (HB) donor (HBD) compounds [1,9-13]; as an

*Abbreviations:* DES, deep eutectic solvent; NADES, natural deep eutectic solvent; HB, hydrogen bonding; HBD, hydrogen bonding donor; Ch, choline; MD, Molecular dynamics; SAXS, Small Angle X-ray Scattering; WAXS, Wide Angle X-ray Scattering; DOSY, diffusion ordered spectroscopy; NOESY, Nuclear Overhauser Effect Spectroscopy; DSC, Differential scanning calorimetry; NMR, nuclear magnetic resonance; ec, Electrical conductivity.

* Corresponding authors at: Istituto Struttura della Materia, Consiglio Nazionale delle Ricerche (ISM-CNR), Rome 00133, Italy (A. Triolo); Department of Chemistry, University of Rome Sapienza, Rome 00185, Italy (O. Russina).

*E-mail addresses:* triolo@ism.cnr.it (A. Triolo), olga.russina@uniroma1.it (O. Russina).

https://doi.org/10.1016/j.molliq.2023.122120
Received 6 March 2023; Received in revised form 12 May 2023; Accepted 14 May 2023
Available online 19 May 2023

example, the stoichiometric ChCl: Urea 1:2 mixture (often indicated as *reline*), is the archetypal DES [1,11-13]. Other commonly encountered Type III DES involve glycerol, ethylene glycol or simple sugars as HBD at given stoichiometric ratios with ChCl.

Using X-ray/neutron scattering and computational tools, fundamental knowledge on the microscopic/nanoscopic organization in these appealing media has been achieved in the last few years [11,14-18]. Neutron scattering studies have been conducted on reline and its microscopic organization has been found to be determined by an intricate blending of large to medium strength HB interactions, with chloride anions wrapped by HB-interacting Ch and urea, in a locally stoichiometrically determined fashion [11,12].

In this intricate scenario, where diverse HB interactions and other interactions (such as coulombic or dispersive ones) are active between different moieties of the DES components, the presence of water has often been considered as potentially detrimental, although the consistent decreasing of viscosity upon water addition can nicely tailor DES properties. Hammond et al. accounted for the role of water addition on the structure of reline [16], together with other groups which focused on this specific system [17,19-21]. The structural effect of water addition to DES [22-24] has also been studied in ChCl:malic acid (1:1, *malicine*) [22-25]. In these studies, water content has been found to be important in affecting DES structural properties and even their structural homogeneity. Small water additions do not affect the resilient DES morphology, thus maintaining a *water-in-DES* situation. However, larger water contents (e.g. 83 mol % in reline) lead to substantial evolution of the solvation shell around DES components, thus leading to the concentration regime of *DES-in-water* [16]. However, the abrupt transition between these two regimes has been recently questioned [26].

Recently, the HBD capability of water was exploited to prepare a NADES, composed solely by ChCl and water, the latter playing the role of a HBD, rather than a contaminant or an additive [27]. Also, we mention that a water-based hydrophobic Type V NADES has been recently proposed as composed by a mixture of thymol and water [28,29].

Concerning the ChCl/water mixture, Zhang et al. explored different mixtures and their thermal characterization could not detect evidences of crystallization, upon cooling for mixtures with water:ChCl ratio, n, between 3.3 and 4.2 [27]. Moreover, based on Brillouin spectroscopy, they proposed the eutectic composition for such a system at ratio n = 4.2. In that study, they also reported density and viscosity data at 25 °C for a series of mixtures with n up to 20 [27].

The system ChCl/water has been further explored, lately. Several studies reported chemical-physical properties of such mixtures, with occasional disagreement between data. ChCl has been reported in the past to form two lower hydrates, a stable di-hydrate and an unstable mono-hydrate [30]. The former compound, with ratio n = 2, melts at 9 °C [30]. Quaternary ammonium salts (such as ChCl) are very efficient in driving strong water structuration around themselves when in aqueous solution [30,31]. In the case of the liquid di-hydrate, Harmon et al. reported IR spectra analogous to other hydrates that are crystalline at ambient conditions (e.g. tetramethylammonium hydroxide pentahydrate) [30]. The same mixture was studied by $^{1}$H NMR and is characterised by very slow proton exchange between choline hydroxyl and water. The authors proposed that choline hydroxyl group is engaged into strong O-H··Cl hydrogen bonds, while the chloride ions are embedded into a framework clathrate by surrounding water molecules [30].

Morrow et al. reported simulations on the liquid structure of two ChCl/water mixtures at two different thermodynamic (p/T) conditions [32]. In those diluted systems (ChCl content was 10 and 20 %wt.), the authors found that both ions are well solvated by water. Shaukat et al. probed hydration and ion association in ChCl dissolved in water, using experimental (dielectric spectroscopy and conductivity) and computational tools probing ChCl in water at infinite dilution [33]. ChCl aqueous solutions have been studied by Vilas-Boas et al., who reported solubility and density data for a series of salts dissolved in water, including ChCl, in the range between 0.1 and 0.3 M fraction, which encompasses the above mentioned eutectic range [34]. We recently reported a structural characterization of a binary mixture of ChCl with water at molar ratio 1:3.3, corresponding to one of the conditions mentioned in ref. [27] as potentially behaving as an eutectic and we indicated such a system as *aquoline*, in analogy to other recently proposed terminologies for ChCl-based DES (e.g. *reline*, *ethaline* and *glyceline*, for ChCl based DES containing urea, ethylene glycol and glycerol, respectively) [35]. ChCl/water mixtures have been studied by other groups as well in the last few years, expanding the range of chemical physical properties explored.

The Solid-Liquid Equilibrium (SLE) in the ChCl/water system has been characterised and discussed by Lobo-Ferreira et al. over the whole concentration range, thus highlighting the existence of an eutectic point with $X_{ChCl} \sim 0.2$ (corresponding to n ~ 4) and $T_{eutect} \sim 204$ K [36]. The corresponding behaviour was previously characterised by other teams. As mentioned, Zhang et al. obtained results in agreement with the above description, in particular they found that mixtures with n = 3.3 and 4.2 behave as good glass formers and no crystallization could be detected for these systems [27]. On the other hand, in 2021, Rahman et al. described thermal transitions in mixtures with n = 3 and 4 at ~194 K [37]. Later Rahman et al. described the thermal behaviour of a wider set of concentrations, confirming these results [38]. We believe that these latter results might have been biased by the experimental conditions chosen for the calorimetric experiments and, as we will show later on, our own characterization confirms the behaviour highlighted by Lobo-Ferreira et al. [36] and Zhang et al. [27].

Density measurements were reported by Zhang et al. at 298.15 K for mixtures with n ranging between 2 and 40 ($0.33 > X_{ChCl} > 0.02$) with density values decreasing, upon water addition from ~1.1 to ~1.0 g/cc [27]. Rahman et al. reported density values between 1.055 and 1.14 g/cc for samples with $1 < n < 10$ ($0.5 > X_{ChCl} > 0.09$) at 295.3 K [38].

Viscosity has also been characterised by different groups. Zhang et al. at 298.15 K explored mixtures with n ranging between 2 and 40 ($0.33 > X_{ChCl} > 0.02$) with viscosity decreasing, upon water addition from ~38 to ~1.0 mPa·s [27]. Rahman et al. reported viscosity values between 100 and 800 mPa·s for samples with $1 < n < 10$ ($0.5 > X_{ChCl} > 0.09$) at 295.3 K [38]. Hirpara, while describing surfactants micellization in aquoline mixtures, reported viscosities ranging between 150 and 180 mPa·s, for mixtures with n = 2–5 (presumably at 303 K) [39]. The latter two data sets indicate a much higher viscosity than the one reported by Zhang et al. and in our present study (that agrees with Zhang et al. values, vide infra). At present, no clear rationalisation for this discrepancy can be proposed.

Despite potential importance as electrolytes for hybrid energy systems [40], concentrated mixtures of ChCl and water have not been explored in detail with respect to electrical conductivity, yet. Quite low conductivity has been reported by Rahman et al. for n = 3 and 4 (3.35 and 3.162 mS/cm, respectively) [38]. Hirpara et al. [39] reported data for n = 2, 3, 4 and 5 in the range between 18.3 and 69.2 mS/cm, which agree with the data that we report in this work. Grishina et al. reported data for n between 2 and 5, as a function of temperature [41]. Finally dilute solutions of ChCl in water have been carefully explored by Shaukat et al. for concentrations n > 20 [42].

Apart from our structural study on a mixture with n = 3.3, which is based on a Molecular Dynamics simulation, only another study focused on the structural organization in water-poor ChCl/water mixtures. Chai et al. reported a study based on the synergy between X-ray scattering and EPSR/DFT computational approaches on four samples with ChCl concentration between 10 and 70 wt% (corresponding to n between 3.3 and 70) [43]. Therein, the role of Hydrogen Bonding (HB) in influencing the structure has been explored.

Other notable reports involving ChCl/water mixtures focused on the utilization of the ChCl/water (n = 3.3) as “formidable green medium enabling the fast activation of reactants” in the synthesis of quinoxalines [44] or on the Molecular Dynamics description of specific applications of ChCl/water mixtures [45,46]. Moreover, Hirpara et al. characterised

surfactants aggregation in aquoline, using a range of complementary experimental techniques [39]. Abbas et al. proposed such mixtures in the framework of the water-in-salt approach to develop electrochemical devices [40].

Overall, the importance of ChCl-rich ChCl/water mixtures is rapidly emerging: a water-based NADES with a wide liquid phase temperature range and tunable chemical physical properties is likely to have a large impact over several applications ranging from extraction to synthesis or catalysis. Accordingly, we undertook a careful investigation of ChCl-rich ChCl/water mixtures, including the (deep) eutectic region, aiming at solving some controversies on selected properties that emerged in the literature and providing an overview of important properties as a ground for further exploration of this class of solvent media. In particular, density, viscosity, electrical conductivity and refractive index were determined over the water:ChCl molar ratio, n, concentration range between 2 and 10 (corresponding to ChCl molar fraction between 0.09 and 0.33) between 275 and 335 K. Moreover, $^{1}H$ and $^{35}Cl$ NMR spectroscopies were applied to determine chemical shifts, relaxation times and choline/water diffusion coefficient as a function of water content. Additionally X-ray scattering was applied to probe the existence of mesoscopic structural organization. In a forthcoming report, MD simulations will focus on rationalisation of X-ray scattering data in terms of both ab initio and classical MD simulations, to account for the complex network of interactions taking place in these mixtures.

## 2. Experimental methods

### 2.1. Chemicals

Choline Chloride (ChCl, Scheme 1) was a TCI-Chemicals product (99.5 %, drying loss: 0.0 %). Before the ChCl/water mixtures preparation, ChCl was dried under high vacuum at 353 K for 96 h to remove residual moisture and then kept in an anhydrous environment. Dried ChCl was weighed in a glove box, and MilliQ water was used to prepare different ChCl/water mixtures. By varying the water content, seven different mixtures with different water:ChCl molar ratios were prepared: n = 2, 3, 4, 5, 6, 7 and 10 (corresponding to molar fraction $0.33 > X_{ChCl} > 0.09$). For selected characterizations, also the sample with n = 20 has been prepared. The mixtures were then kept at ca. 325 K under constant agitation to obtain transparent and homogenous liquids. Mixtures prepared in such a way were sealed and maintained at ambient conditions until ready for further characterizations.

### 2.2. DSC measurements

Thermograms were collected using a Mettler Toledo DSC 822 equipped with an FRS5 sensor and a liquid nitrogen cooleing system. During the measurements, the furnace was purged with dry nitrogen at a flow rate of 30 ml·min$^{-1}$. Samples were weighed using a Mettler MT5 analytical balance (uncertainty of 0.005 mg) in a range between 4 mg and 6 mg, and then they were placed in a 40 μl aluminium pan and rapidly sealed. Therefore, the mixtures were subjected to a temperature program that provided a dynamic cooling from 25 °C to −100 °C at 5 °C/min, followed by a heating from −100 °C to 40 °C, with a scanning rate equal to 5 °C/min.

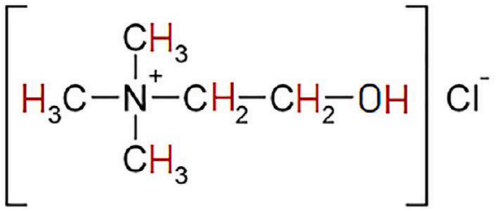

**Scheme 1.** Schematic representation of Choline Chloride.

### 2.3. Density measurements

Density (ρ) was determined using a Mettler Toledo Density Meter DM45 DeltaRange in the temperature range from 278.15 K to 333.15 K, after a calibration procedure conducted using dry air and bi-distilled water at 293.15 K.

### 2.4. Viscosity measurements

Dynamic viscosity (η) values were obtained using an Anton Paar micro viscosimeter (model Lovis 2000 M/ME, with accuracy up to 0.5 %) based on Peltier elements (accuracy of 0.02 K) and using calibrated glass capillaries with different diameters (1.59 mm, 1.80 mm and 2.50 mm, depending on the probed viscosity range). Measurements were conducted in the temperature range between 283.15 K and 323.15 K.

### 2.5. Electrical conductivity measurements

The electrical conductivity (ec) was measured between 278.15 and 313.15 K, using a Mettler Toledo Five Easy FE30 conductivity meter, which operates with a LE703 conductivity electrode, with a 0.73 cm$^{-1}$ cell constant. Temperature was controlled with a thermostatic bath with an uncertainty of 0.1 K.

### 2.6. Refractive index

An Abbe Refractometer 2AWJ (Optika) was employed to determine the refractive index ($n_D$) at the Na D line (589 nm). It is equipped with a thermostat to cover the temperature range from 273.15 K to 343.15 K. It can measure refractive indices between 1.3 and 1.7 with a resolution of 0.0005. Measurements were conducted each 10 K in the temperature range from 293.15 K to 323.15 K.

### 2.7. Small and Wide Angle X-ray Scattering

Small Angle X-ray Scattering (SAXS) measurements were performed at the SAXSLab Sapienza with a Xeuss 2.0 Q-Xoom system (Xenocs SA, Sassenage, France), equipped with a micro-focus Genix 3D X-ray source (λ = 0.1542 nm), a two-dimensional Pilatus3 R 300 K detector which can be placed at variable distance from the sample. Calibration of the scattering vector Q range, where $Q=(4\pi \sin\theta)/\lambda$, 2θ being the scattering angle, was performed using a silver behenate standard. Measurements with different sample-detector distances were performed so that the overall explored Q region was $0.1 < Q < 3.3$ Å$^{-1}$. The samples were loaded into a disposable quartz capillary with nominal thickness 1.0 mm and sealed with hot glue before placing them in the instrument sample chamber at reduced pressure (~0.2 mbar). The two-dimensional scattering patterns were subtracted for the dark counting, and then masked, azimuthally averaged and normalized for transmitted beam intensity, exposure time and subtended solid angle per pixel, by using the FoxTrot software developed at SOLEIL. The one-dimensional S(Q) vs. Q profiles were then subtracted for the capillary contribution. The measurements were conducted at ambient temperature (ca. 293 K) on samples with n = 2, 3 and 4, which maintained liquid and homogeneous during the whole length of the experiment.

Wide Angle X-ray Scattering (WAXS) data on samples with n = 2, 3 and 4 were collected at room temperature (ca. 293 K) using the non-commercial Energy Dispersive X-ray Diffractometer (EDXD) built in the Department of Chemistry, Rome University "Sapienza" (Italian Pat. Appl. no. 1126484–23 June 1993).White Bremsstrahlung radiation emitted by a tungsten tube (50 kV, 40 mA) was used. The scattering variable Q (transferred momentum) is given by: $Q$ (Å$^{-1}$) $= 4\pi/\lambda_i \sin\theta = E_i \sin\theta$, where $E_i$ is the beam component energy (in keV) and θ is the scattering angle. Using a white beam, data were collected at different θ values (namely: 1°, 3°, 8° and 22°) with an energy sensitive, high purity, solid-state Ge detector. Data were corrected for absorption and

background and white beam scattering using in house developed software [47,48] and eventually were merged to yield the total static structure factor, P(Q):

$$P(Q) = I_{e.u.}(Q) - \sum_{i=1}^{n} x_i f_i(Q)^2$$

where $f_i(Q)$ are the interpolated atomic scattering factors, $x_i$ are the number concentrations of i-type atoms in the stoichiometric unit, and $I_{e.u.}(Q)$ is the observed intensity in electron units.

Samples were contained in quartz capillaries of 2 mm diameter.

### 2.8. NMR spectroscopy

ChCl/water samples were transferred to 5 mm NMR tubes, equipped with a capillary containing a solution of NaCl 0.5 M in deuterated water ($D_2O$) used as chemical shift reference and for lock. $^1$H NMR experiments were carried out on a Bruker NEO 500 console (11.74 T) equipped with a 5 mm broadband inverse probehead. The diffusion ordered spectroscopy (DOSY) experiments were performed using the bipolar pulse-longitudinal eddy current delay (BPP-LED) pulse sequence with the following parameters: pulse gradient $\delta = 1.5$–3 ms, diffusion time $\Delta = 0.1$–0.5 ms, 8 scans, and a relaxation delay of 10 s. The pulse gradients were incremented from 2 to 95% of the maximum gradient strength in a linear ramp with 32 steps. A pulsed gradient unit capable of producing sine-shaped magnetic field pulse gradients in the z-direction of 53 G cm$^{-1}$ was used. The spin-lattice relaxation times ($T_1$) were measured using the inversion recovery (IR) pulse sequence. All spectra were recorded for various delay time $\tau$, in the range 0.05–18 s with data matrices of 16,384 (t2) × 16 (t1) complex data points over a spectral width of 9 ppm. The temperature was set at 300–330 K and controlled with an airflow of 535 l h$^{-1}$.

The two-dimensional homonuclear $^1$H–$^1$H NOESY correlation experiments were recorded with a sweep width of 9 ppm, 8 scans for each of the 512 increments (F1), 4096 (F2) and a mixing time of 50 ms.

$^{35}$Cl experiments were carried out on a Bruker Avance 500 spectrometer operating at a Larmor frequency of 500.13 MHz for $^1$H and 49.002 for $^{35}$Cl. The spectra were collected with standard 1D acquisition sequences, using a ARING pulse train to reduce acoustic ringing artefacts, a relaxation delay of 1 s and 16 scans. Samples were analyzed at 300–330 K and the temperature was controlled within 0.1 K with a BVT3000 variable temperature unit.

## 3. Results and discussion

The thermal behavior of the probed ChCl/water mixtures is presented in Fig. 1. These data look in agreement with corresponding data sets from previous reports from Zhang et al. [27] and Lobo Ferreira et al. [36]; on the other hand these traces looks in disagreement with the characterizations from Rahman et al. [37,38]. The origin of these discrepancies is not clear. Mixtures with n = 2, 5, 6, 7, and 10 are characterised by endothermic first-order transitions during heating, which can be attributed to the melting of crystalline phases. Mixtures with n ≥ 5 show a melting point, $T_m$, lower than 273.15 K, that is below the ones of both neat components. Samples with n = 2 and 5 show a cold crystallization event ($T_{cc}$), an exothermic process observed upon heating the samples. It is important to highlight that in the case of mixtures with n = 3 and 4, no thermal transition could be detected; this range corresponds to the regime where Lobo Ferreira et al. determined the existence of an eutectic ($x_{ChCl} = 0.2$, n = 4) [36]. Analogously Zhang et al. observed no transitions for n = 3.3 and 4.2 [27]. $T_m$ and $T_{cc}$ values derived from data of Fig. 1 are listed in **Table S1** of the ESI.

In Fig. 2, the melting temperatures are shown to highlight the Solid-Liquid Equilibrium (SLE) conditions, together with corresponding available data from Zhang et al. [27] and Lobo-Ferreira et al. [36] Ideal SLE curves are also reported on the basis of the relationship:

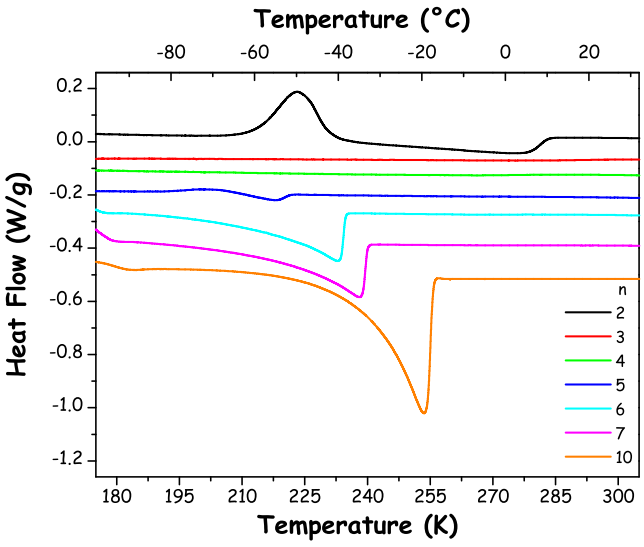


**Fig. 1.** DSC thermograms of ChCl/water mixtures at different molar ratios n obtained upon heating at 5 K/min. Data are arbitrarily vertically shifted, for clarity.

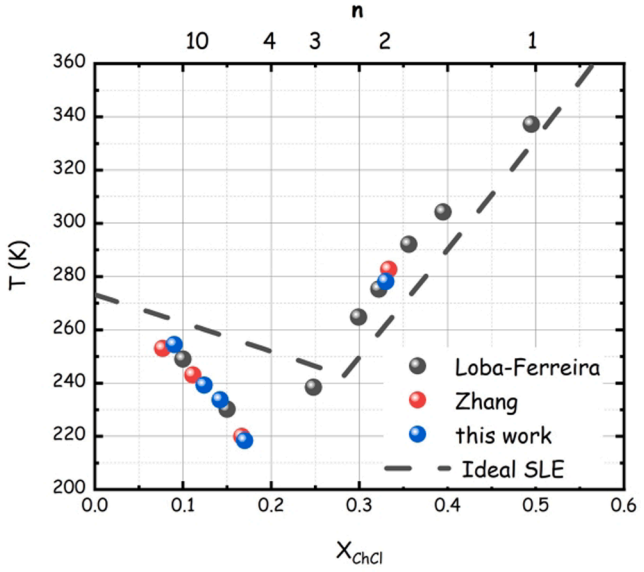


**Fig. 2.** Solid-liquid equilibrium diagram for ChCl/water mixtures (this work, blue symbol). Data for n = 2, 5, 6, 7, 10 are shown. Corresponding data sets from Zhang et al. (red symbol) and Lobo-Ferreira et al. (black symbol) are included for comparison. Ideal SLE data are reported as well (dashed line). (For interpretation of the references to colour in this figure legend, the reader is referred to the web version of this article.)

$$T_i = \frac{T_{m,i}\,\Delta_{fus}H_i}{\Delta_{fus}H_i - RT^{*}lnx_i} \quad (1)$$

where the ideal (considering that both components have unitary activity coefficients in the mixtures) melting temperature of the i-th component, $T_i$, is evaluated in terms of its enthalpy of fusion ($\Delta_{fus}H_i$), melting temperature ($T_{m,i}$) and molar fraction ($x_i$) in the mixture [49]. Therein, parameters for ChCl are used from the recent work by Fernandez et al. [49], while, parameters from water are derived from Osborne [50]. Equation (1) assumes that $\Delta_m Cp_i$ (the difference between molar heat capacity of the i-th component in the liquid and solid phases) is negligible compared to the rest of the contribution.

Accrding to these latter studies, the system ChCl/water presents an eutectic composition close to $x_{ChCl} = 0.2$ and an eutectic temperature of T = 218.35 K [49]. We notice that similarly to other related works, in our characterization, no first order transition can be detected for samples with n = 3 and 4 ($x_{ChCl}$ = 0.25 and 0.2, respectively), although Lobo-Ferreira et al. [36] report a melting point for the n = 3 sample.

In Fig. 2, we observe that our results, analogously to results from other teams [27,36], indicate positive deviations of melting points with respect to the ideal behaviour in ChCl-rich mixtures (this behaviour was mentioned, when dealing with ChCl/Urea mixtures and rationalised in terms of the existence of non-negligible $\Delta_m Cp_i$ terms [51]). On the other hand, a distinct negative deviation is observed in water-rich regimes ($x_{ChCl} < 0.25$), suggesting that the interactions water–ChCl are significantly stronger than water-water ones. A melting temperature for samples with n ~ 4 ($x_{ChCl} = 0.2$) cannot be detected in all these studies and a glassy state is achieved before crystallization occurrence. Even subsequent heating does not lead to cold crystallization events at this concentration. Considering the ideal location of the eutectic concentration ($x_{ChCl}$ ~ 0.28, n ~ 2.6; T ~ 240 K), although the melting point of the sample with $x_{ChCl} = 0.2$ (n = 4) cannot be detected, we can yet consider this concentration as representing the DES condition for the ChCl/water system, hence indicating this mixture as *aquoline*.

Density values for the probed ChCl/water mixtures are shown as a function of temperature in the range between 278.15 K and 333.15 K in Fig. 3 (the corresponding data set is reported in **Table S2** of the ESI). The temperature dependence of density was modelled with the following equation:

$$\rho(T) = AT^2 + BT + \rho_o \quad (2)$$

where ρ ($g \cdot cm^{-3}$) denotes the density of the samples. Parameters A, B and $\rho_o$ are fitting parameters and their values for each n are reported in the Supporting Information (**Table S3**). Some groups reported a linear trend for ρ(T) in many DESs based on ChCl (particularly reline) that nicely accounts for the data, especially if collected over limited temperature windows [52-50]. In this study, the relatively large temperature window accessed for the measurements leads to better quality modelling when using a quadratic form of ρ(T), similarly to Yadav [55] and Agieienko [56]. Indeed, previous studies of the ChCl/water system highlighted a quadratic temperature dependence for density in the range of 278.15 K-318.15 K [33].

Density values at 298.15 K are reported as a function of n in the ESI, (**Figure S1**). By increasing the n ratio, density decreases with a monotone trend that can be modelled with a first order exponential decay empirically determined as:

$$\rho_{298.15K} = A_1 + A_2 \bullet e^{-\frac{n}{A_3}} \quad (3)$$

with parameters reported in the ESI (**Table S4**).

Although water represents one of the main components in the presently considered mixtures, it is meaningful to compare the present results with those for DESs based on ChCl and another HBD, where the effect of deliberate water additions was investigated, in terms of density. Lapena et al. reported that for aqueous ChCl:Urea 1:2, the density of the hydrated mixtures was lower than that of the pure DES [57]. The density of ChCl based DESs (with oxalic acid, levulinic acid, glutaric acid, malonic acid, and glycolic acid as HBD) saturated with water (5%) was lower than that of the dried DESs [58]. Finally, a nonlinear increase in the density with ChCl molalities at a given temperature in dilute aqueous mixtures of choline chloride was observed [42].

The thermal expansion observed in the samples, upon increasing the temperature, is best quantified by the volumetric isobaric thermal expansion coefficient $\alpha_P$, which is defined as:

$$\alpha_P = -1/(\rho(T)) \bullet ((\partial \rho(T))/\partial T)_P \quad (4)$$

Considering the quadratic model employed for ρ(T), this coefficient can be determined as follows:

$$\alpha_P = -(2 \cdot A \cdot T + B)/(A \cdot T^2 + B \cdot T + \rho_0) \quad (5)$$

The volumetric thermal expansion coefficient is related to the temperature dependence of the separation distance between the atoms or the molecules that constitute a sample. For all the investigated mixtures, the thermal expansion coefficient shows a monotone increase with temperature, whose slope becomes steeper as the water content increases, tending to the water behaviour (Fig. 4, the corresponding data are reported in **Table S5** of the ESI). It is reasonable to envisage that specific ChCl/water interactions lead to "rigid" and local structures that persist across the explored temperature range and whose rigidity is higher at lower water content and decreases upon heating. In this context, it is noteworthy the existence of a temperature (ca. 315 K), where the different $\alpha_P$ curves cross each other. Such a behavior is likely related to that observed in neat water, whose thermal expansion coefficient $\alpha_P(T,P)$ was determined as a function of temperature for several different pressures in the range 1 bar − 8 kbar. In this case, the different isobar curves cross at a temperature value T* = 315 K, which represents the low temperature onset for the establishment of patches of local and

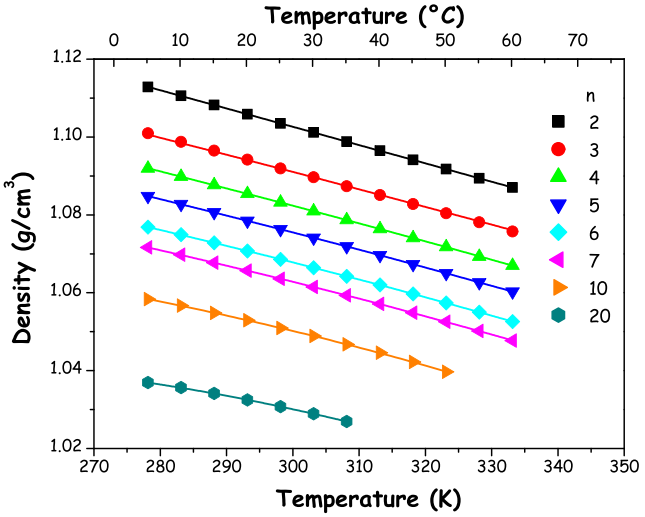


**Fig. 3.** Density of ChCl/water mixtures at different water:ChCl ratios n. The solid lines represent the description of experimental data in terms of equation $\rho(T) = AT^2 + BT + \rho_o$.

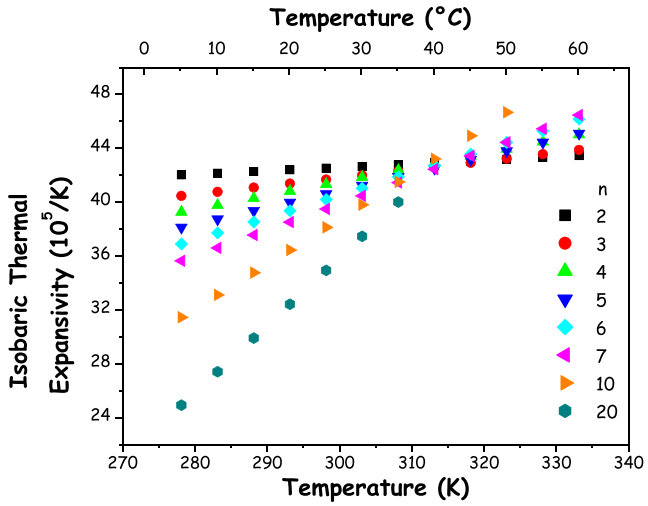


**Fig. 4.** Isobaric Thermal Expansivity as function of temperature between 278.15 K and 333.15 K for the probed ChCl:W mixtures at different water:ChCl molar ratios n.

transient tetrabonded HB network for water [59].

Dynamic viscosity values η (mPa·s) of ChCl/W mixtures were obtained in the temperature range from 283.15 K to 323.15 K. In Fig. 5, the experimental data are reported (data are listed in **Table S6** in the ESI) and described in terms of the Vogel-Fulcher-Tamann model:

$$ln\eta = ln\eta_0 + \frac{D}{T - T_0} \quad (6)$$

where $\eta_0$, $T_0$ and D are fitting parameters and are listed in **Table S7** in the ESI.

The fitting parameters D and $T_0$ were used to derive the energy of activation for viscous flow, $E_{a,\eta}$, at T = 298.15 K (Fig. 6) via the expression:

$$E_{a,\eta} = R\frac{dln\eta}{d(\frac{1}{T})} = RD(\frac{T}{T - T_0})^2 \quad (7)$$

where, R is the gas constant. $E_{a,\eta}$ represents the energy barrier that a specimen (molecule or ion) must overcome when subjected to a viscous flow at 298.15 K and is a measure of how rapidly viscosity changes with temperature [60]. By increasing the water content, the energy barrier related to the resistance of the mixtures to flow is found to decreases.

At 298.15 K, the viscosity decreases upon increasing water content (as shown in **Table S8** and **Figure S2** in the ESI), as observed for other ChCl aqueous solutions: Zhang et al. explored the range between n = 2 and 18 at 298.15 K and obtained data in very good agreement with the present study [27]. Shaukat et al. reported that dynamic viscosity values of aqueous solutions of ChCl with solute molalities ≤ 2.0 mol/kg decreased with the solute molalities, which are in agreement with our trend [42]. On the other hand, recent reports from Rahman et al. [38] and Hirpara et al. [39] indicate a much higher viscosity (>100 mPa s) for the water content covered by this study and a clear rationalisation for these observation is missing. It is noteworthy that at 298.15 K ChCl/water mixtures show viscosity values much lower than other common DES, such as reline [57].

Electrical conductivity (ec) of ChCl/W mixtures were obtained in the temperature range from 278.15 K to 313.15 K, every 5 K. In Fig. 7, the experimental data are reported (data are listed in **Table S9** in the ESI) and described in terms of κthe Vogel-Fulcher-Tamann model:

$$\ln \kappa = \ln \kappa_o + D_\kappa/(T\text{-}T_\kappa) \quad (8)$$

where $\kappa_o$, $T_\kappa$ and $D_\kappa$ are fitting parameters and are listed in **Table S10** in the ESI.

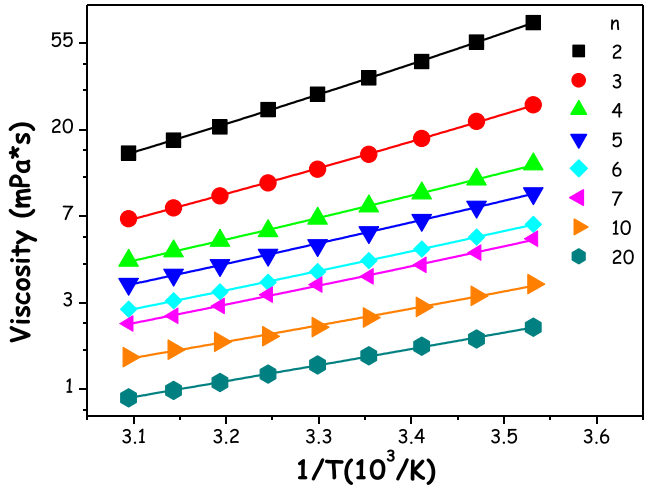


**Fig. 5.** Dynamic viscosity η (mPa·s) of ChCl/water mixtures at different ratios, n, as a function of temperature. Solid lines represent the description in terms of the VFT model.

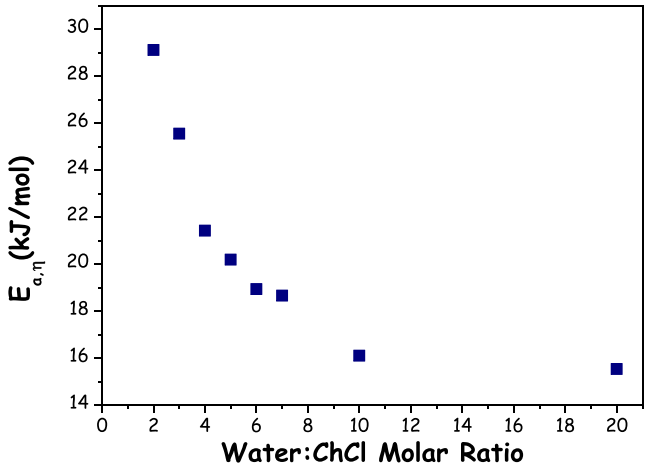


**Fig. 6.** Energy of activation for viscous flow as a function of n for the probed ChCl/water mixtures at 298.15 K.

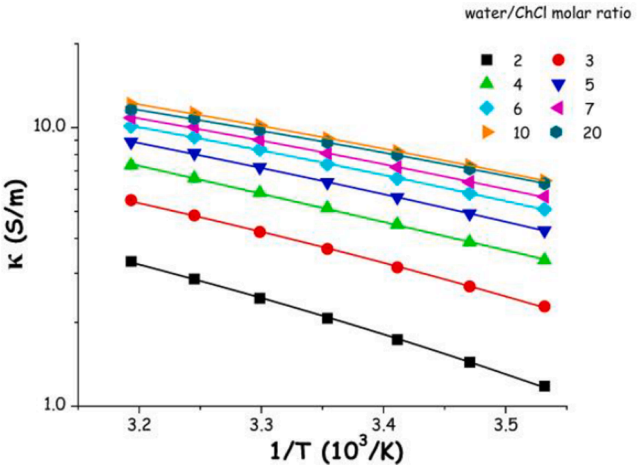


**Fig. 7.** Electrical conductivity, κ, ($S \cdot m^{-1}$) of ChCl/water mixtures at different ratios, n, as a function of temperature. Solid lines represent the description in terms of the VFT model.

A comparison between ec data collected in the present work and literature data set at 25 °C is shown in Fig. 8, as a function of molality. Therein, data from Shaukat et al. [42] at more diluted concentrations are shown. Our data look in good agreement with ref. [42] and confirm the existence of a maximum in electrical conductivity at ca. 4 m (corresponding to ca. n = 15). Data were modelled in terms of the Casteel-Amis equation:

$$\kappa = \kappa_{max}\left(\frac{m}{m_{max}}\right)^a exp\left[-bm_{max}^2\left(\frac{m}{m_{max}} - 1\right)^2 - a\left(\frac{m}{m_{max}} - 1\right)\right] \quad (9)$$

where $\kappa_{max}$ is the maximum ec obtained at molal concentration $m_{max}$, a and b fitting curve shape parameters. The fitting parameters are reported in **Table S11** of the ESI, and, reflecting the wider concentration range covered, are slightly different from those reported earlier [42].

The relationship between electric conductivity and viscosity in the present series of mixtures was probed. Molar conductivity ($\Lambda = \kappa \cdot M/\rho$, where M is the mixture molar mass and ρ is the density) is plotted in Fig. 9 versus fluidity, in order to probe the Walden product [61,62]. Such a representation delivers information on the degree of ionic dissociation in the mixture, as compared to an ideal reference trend, corresponding to dilute aqueous KCl solutions (where independent ions without any interionic interactions are assumed to be present). The

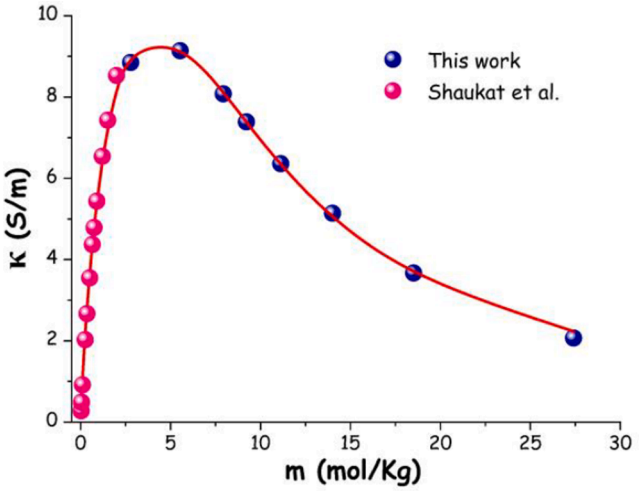


**Fig. 8.** Electrical conductivity, κ, ($S \cdot m^{-1}$) of ChCl/water mixtures at different ratios, n, as a function of molal concentration, as obtained in this work and in the work by Shaukat et al. [42] at 298.15 K. The solid line represents the global description in terms of the Casteel-Amis equation.

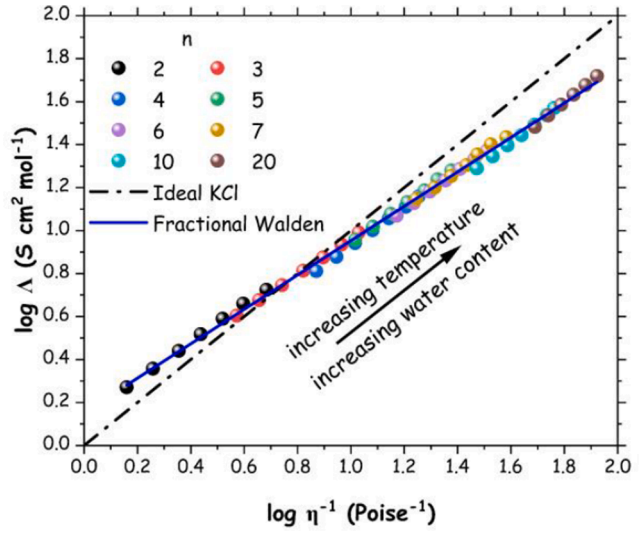


**Fig. 9.** Walden plot (log molar conductivity vs. fluidity) of ChCl/water mixtures at different ratios, n. The dashed line represents the ideal trend for a 0.01 mol/L aqueous KCl solution; the continuous line represent a global linear fit of all data to highlight the decoupling behaviour (see the text).

trend reported therein indicates that for all water content a *good ionic* behaviour is found with small deviations from the ideal trend. This behaviour reminds of the ChCl-Urea (1:2, reline) mixtures with water studied by Agieienko et al. [56], where neat reline and its water mixtures showed a good ionic liquid behaviour, as well. Also in that case a slight deviation from ideal trend was observed; here we modelled the non ideal trend in terms of the behaviour $\Lambda\eta^{\alpha} = cost$, where α is inversely proportional to the decoupling index, $R_{\tau}$, introduced by McLin et al. [63] to account for decoupling between shear and conductivity relaxation times. Here, the observed trend can be described with $\alpha = 0.80$ that nicely accounts for both water content and temperature increase effects and reflects the result the onset of correlation in ionic positions. Overall, the observed Walden plot for ChCl/water systems reflects a *good ionic* liquid behaviour that can be compared with the *poor ionic* liquids behaviour claimed in [62] and the *good ionic* liquids behaviour reported in [64] for different ChCl-based DES.

The refractive indices $n_D$ of ChCl/water systems were measured each 10 K in the temperature interval ranging from 293.15 K to 323.15 K. The experimental results are shown in Fig. 10 and listed in (**Table S12** in the ESI). The experimental data were modelled with a linear trend and the corresponding parameters are reported in the ESI (**Table S13**). For several DESs, the $n_D$ -T relationship has been reported to be linear [65,66].

At a given temperature (e.g. 293.15 K), $n_D$ decreases upon increasing water content (see **Figure S3** in the ESI). Moreover a linear trend could be observed for $n_D$ vs. ρ, as exemplified in Fig. 11 for the case of T = 293.15 K.

$^1$H NMR spectroscopy has been shown to efficiently monitor the nature of solvation and structural organization when adding water to DES and in the case of ChCl/water mixtures [27,63-66]. Harmon et al. showed the slow, or even absent, proton exchange between water protons and choline hydroxyl group one, on the time scale of NMR experiments, in the case of water-poor mixtures. Only above n = 6, the two signals for the different protons merged into a unique feature that fingerprints the fast exchange between the two protons at the NMR time scale. This was interpreted as the consequence of a tight correlation between chloride ion and water, leading to a rigid clathrate-like cage around choline's hydroxyl group: only above n = 4.5 such a rigid cage expands and allows water-choline hydroxyl group interaction [67]. Another recent study accounted for HDO/$H_2O$ peak chemical shift in ChCl/water mixtures [27], revealing an abrupt change in this quantity across ca. n = 5. Here we monitored $^1$H and $^{35}$Cl chemical shifts and line widths for the different protons in the ChCl/water mixtures and for Cl at 300 K and 330 K. The measured $^1$H spectrum of samples with n between 2 and 20, acquired at 300 K, are reported in the ESI (**Figure S4**), while in Fig. 12 **a)**, we report the trend for $^1$H chemical shifts of the different moieties as a function of n. Upon increasing water content, the chemical shift and line width of –OH and $H_2O$ signals progressively evolve: downfield shifts occur signals, suggesting the development of a stronger hydrogen bonding network, similarly to results in related systems [71]. It emerges that above n = 6, coalescence of the –OH/ $H_2O$ peaks in a broad signal manifests suggesting that fast exchange gets activated at 300 K, while for n in the range 2–5 still a slow to intermediate dynamic exchange regime is observed. Moreover, small to negligible changes are observed for $CH_3$ and $CH_2$(2) protons, while a distinct downfield trend is found for $CH_2$(3) protons. The clearest transition is however observed for $H_2O$ $^1$H chemical shift, with a transition at n ~ 5. Increasing the temperature at 330 K an up-field shift is observed for –OH and $H_2O$ signals, indicating a weakening of the HB network.

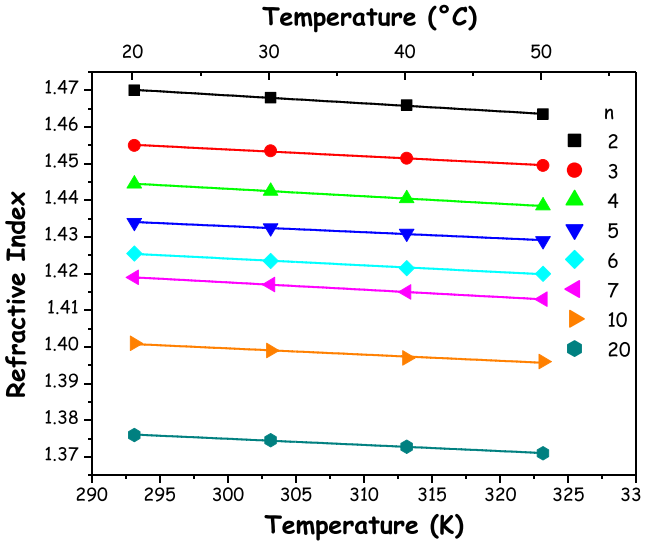


**Fig. 10.** Refractive index, $n_D$, as a function of temperature for the probed ChCl/water mixtures. Linear fits are reported.

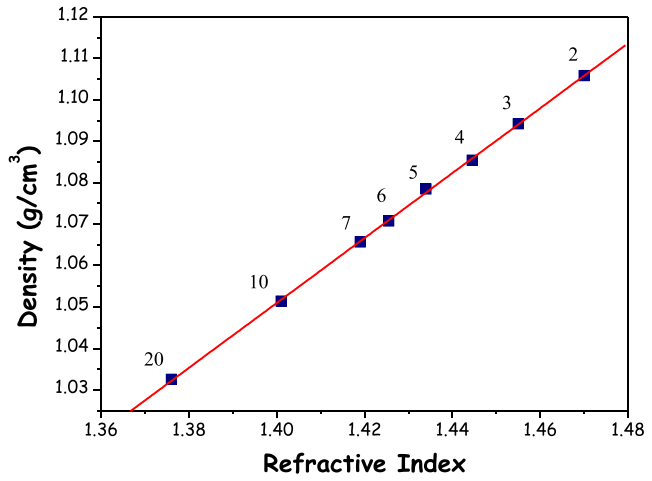


**Fig. 11.** Linear dependence between density and refractive index $n_D$ at 293.15 K, as ChCl/water molar ratio n varies.

We also show $^{35}$Cl NMR spectra for different mixtures in the ESI (**Figure S5**), while in Fig. 12 **b)**, we show the water content dependence for the chemical shift of the peak, as a function of n. A $^{35}$Cl upfield chemical shift of ~23 ppm is observed, upon decreasing the amount of water. This shift indicates larger shielding of chloride anion upon dilution, consistent with the stronger chloride-water interaction. Moreover, $^{35}$Cl peak lineshape (data provided in the ESI: **Table S15**) provides information about chloride anion environment and hydration. In $^{35}$Cl spectra, narrow lineshapes, due to small quadrupolar coupling constant, are observed for highly symmetric environment such as NaCl dissolved in a diluted water solution [72,73]; in our samples, upon decreasing the water content, a symmetry decrease of the chloride anion environment is observed, as indicated by the progressive increase of the quadrupolar coupling constant/line width [74]. Finally, experimental linewidths at half height (FWHM) of the $^{35}$Cl peaks are related to the relaxation times ($T_2$) which are listed in the ESI in **Table S15**). As expected, from the linewidth analysis, the $T_2$ value increases with water addition indicating again a progressive more symmetric hydration shell surrounding the chloride anion until a chloride-in-water solution is observed for n = 20. In particular, the graph of $T_2$ as a function of n (**Figure S6** in the ESI) shows two trends: a steep initial increase for n = 2–5 followed by a less pronounced variation for the ChCl/water systems with n = 6–20.

The NMR technique was also exploited to extract dynamic information in the ChCl/water mixtures. In fact, NMR diffusion studies offer molecular level information on the translational motion of the individual species, whereas the rotational information at the atomic level can be obtained from NMR relaxation studies.

Two separate peaks are observed in the DOSY map at T = 300 K (data not shown). One peak can be attributed to $H_2O$-OH and the other to the choline ion. The hydroxyl proton of choline diffuses faster than rest of the molecule and such a difference is due to the dynamic exchange with water during the diffusion time (see e.g. [75]). The diffusion coefficients of both choline and –OH/ $H_2O$ (shown in the **Table S16** in the ESI and in Fig. 13 **a)**) increase with the amount of added water, this reflects the decrease in viscosity of the whole system. Considering the Stokes-Einstein relationship between diffusion coefficient and inverse viscosity, namely:

$$D = \frac{k_B \bullet T}{6\pi \bullet \eta \bullet R} \tag{10}$$

where $k_B$ is the Boltzmann constant, T = 300 K is the measurements temperature, η is the viscosity and R the hydrodynamic radius of the diffusing object, one obtains the plot in Fig. 13 **b)**, where a distinct linear dependence exists between the two properties for choline, with a best fit value of hydrodynamic radius equal to 4.2 Å [10,75].

In **Figure S7** (in the ESI) we report the longitudinal (spin lattice, $T_1$) relaxation time for proton, that provides information about the intra and intermolecular relaxation mechanisms of each spin in a given molecule and thus is an indicators of the rotational mobility. The $T_1$ relaxation times of all protons of the system choline/water were measured at 300 K and reported in **Table S17** in the ESI. The measured $T_1$ of all protons in ChCl/water mixtures increase upon water addition, thus a progressively fast rotational motion is observed. The $T_1$ of the methyl group are less affected by the water content, which is also correlated with the unchanged proton chemical shift with addition of water.

Furthermore, 2D NOESY experiments were performed to investigate choline-protons/water spatial proximity (≤5 Å) increasing the amount of added water (n = 2, 4). The NOESY spectrum for the system with n = 2, displayed in Fig. 14, shows intermolecular NOE cross peaks between both choline hydroxyl/methyl groups and water protons, while no correlation peaks are observed for the aliphatic $CH_2$ protons with water. Similar results are obtained for the system choline/water n = 4 (see **Figure S8** in the ESI). A qualitative interpretation of the NOESY data allows sketching the solvation of choline groups (see Scheme in Fig. 14) with water molecules located primarily in the proximity of the methyl and hydroxyl groups. This picture agrees with the bimodal solvation model arising from our previous work on ChCl/water with n = 3.3 [35].

The structural organization in ChCl-rich mixtures was monitored using Small-Wide Angle X-ray Scattering (SWAXS), aiming at detecting the potential presence of large-scale aggregates that might characterised the morphology of such systems. Fig. 15 shows SWAXS data from samples with n = 2, 3 and 4 at 20 °C. Therein it emerges that for Q values higher than ca. 5 Å$^{-1}$, the diffraction patterns do not appreciably differ, while non-negligible differences appear below that Q value, fingerprinting differences in local structure due to water content variations. While these patterns will be studied in detail in a forthcoming report, related X-ray scattering data sets have been recently published and modelled with Reverse Monte Carlo techniques, although not full

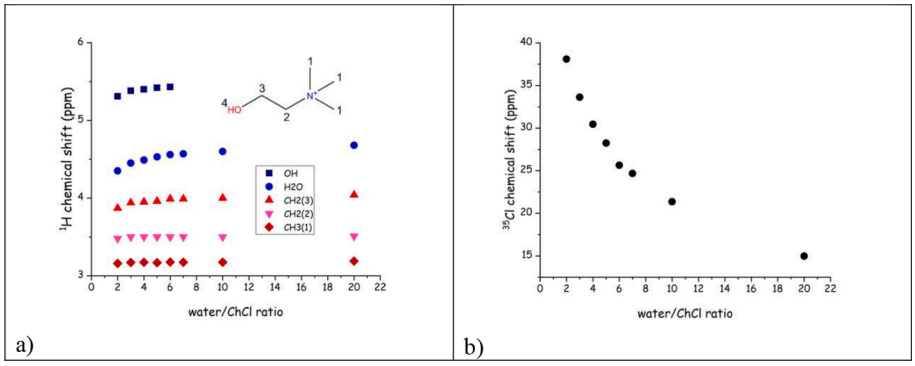


**Fig. 12.** a) $^1$H and b) $^{35}$Cl chemical shifts of the different moieties in ChCl/water as a function of n, at 300 K. Proton nomenclature is illustrated in the inset.

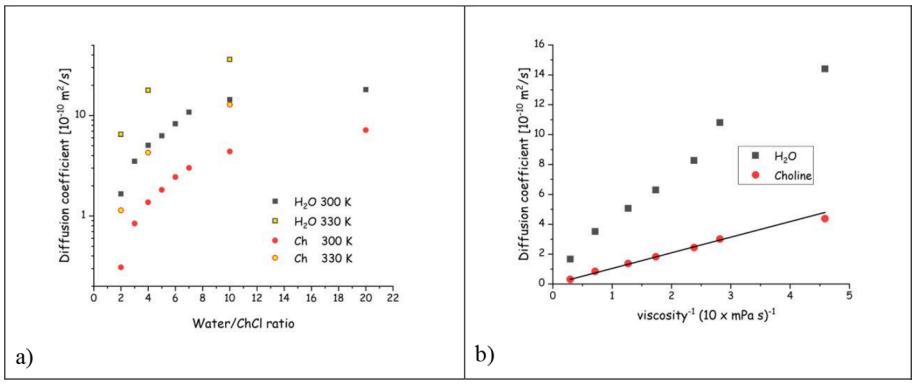


**Fig. 13.** a) Diffusion coefficients for water (squares) and choline (circles) in ChCl/water as a function of n, at 300 (filled symbols) and 330 K (yellow filled symbols). b) Diffusion coefficients for water (squares) and choline (circles) in ChCl/water as a function of inverse viscosity for the different ChCl/water mixtures at 300 K. The line corresponds to a fit of data in terms of the Stokes-Einstein equation. (For interpretation of the references to colour in this figure legend, the reader is referred to the web version of this article.)

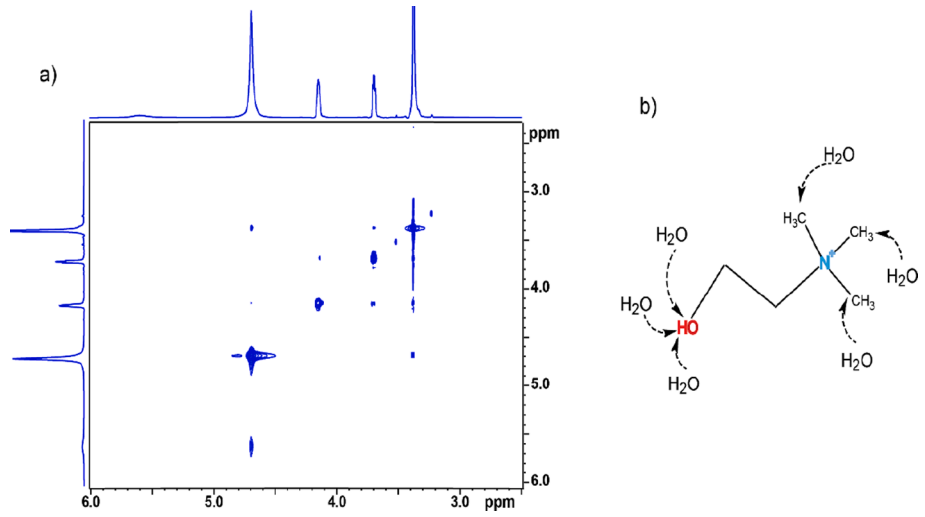


**Fig. 14.** $^{1}H$–$^{1}H$ NOESY spectrum of choline/water (n = 2) sample acquired at 300 K with mixing time of 50 ms.

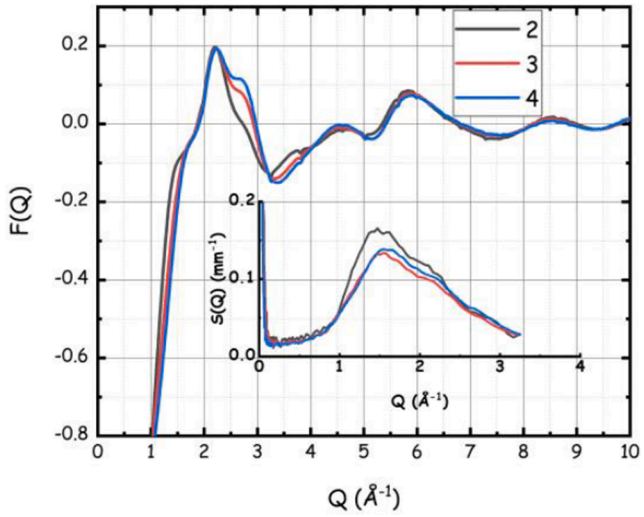


**Fig. 15.** Wide Angle X-ray Scattering from samples with water:ChCl ratio, n, equal to 2, 3 and 4 at ambient conditions. In the inset the Small Angle X-ray Scattering data from the same samples are shown.

account for the low Q portion was achieved with this tool [43]. In the inset of the figure, the Small Angle X-ray scattering data set is shown for the same samples, showing that no low Q scattering features can be detected below 1 $Å^{-1}$, thus indicating that no large aggregates exist even in the case of di-hydrate sample and only a progressive change of peaks features can be observed.

## 4. Conclusion

Aiming at the exploitation of performance tunability of Deep Eutectic Solvents and their eco-sustainability, a constant evolution in the chemical properties of the DES components is presently witnessed. Natural DES are likely among the preferred class to be probed for appealing properties, due to their limited environmental impact. Water-based NADES represent then a key class of solvents that might prove tunable enough for sustainable development in a variety of fields.

In this respect, Choline Chloride/water mixtures represent then an archetypal example of potentially interesting new solvent media and results shown in the recent literature and integrated with the present experiments indicate that a wide tunability of chemical-physical properties can be achieved by limited changes in water content.

The depicted scenario calls then for a wide set of experimental data to fully uncover the potential of this class of systems. With this perspective we undertook an extended characterization of chemical-physical properties of ChCl/water mixtures, aiming at: a) characterising the solid-liquid equilibrium and clarify matters on the existence and nature of the deep eutectic condition; b) exploring diverse properties (density, viscosity, refractive index, morphology, $^{1}H$ NMR diffusion coefficient and NOESY) across the mentioned deep eutectic concentration and c) understanding if the mentioned properties can be efficient indicators of the occurrence of a deep eutectic condition.

By integration of literature calorimetric data and our present data

set, it is possible to confirm that the concentration regime corresponding to n = 3–4 is characterised by a strong tendency to supercool into a glassy state, thus hindering the accurate determination of the melting point. Nevertheless, the shift both in concentration and in melting point with respect to the ideal behaviour for the ChCl/water mixture clearly supports the DES nature of the mixture corresponding to n ~ 4 (aquoline).

A large set of experimental data has been obtained typically in the range $2 \leq n \leq 10$ and $280 \leq T(K) \leq 320$, accessing volumetric, viscous, optical, dynamic and structural information, complementing and extending the literature data sets.

Overall, the extended amount of experimental data sets do not show abrupt changes when approaching the deep eutectic concentration, apart from gradual monotone evolution with water content and only the thermal characterization can access specific features that can be associated to the drop in melting at particular concentration regime.

In perspective, the role of water-based NADES is expected to widen and provide new solutions for technologically relevant problems; accordingly, a more detailed comprehension of the aquoline system would provide benefit to enlarge the range of applications. Atomistic description of microscopic features leading to macroscopic performances will then be pursued in the near future by integration of X-ray and Neutron scattering supported by Molecular Dynamics simulations.

*CRediT authorship contribution statement*

**Emanuela Mangiacapre:** Investigation, Data curation, Writing – original draft. **Franca Castiglione:** Investigation, Data curation. **Matteo D'Aristotile:** Investigation, Data curation. **Valerio Di Lisio:** Investigation. **Alessandro Triolo:** Conceptualization, Investigation, Formal analysis, Funding acquisition, Writing – original draft, Writing – review & editing. **Olga Russina:** Investigation, Supervision, Funding acquisition, Writing – review & editing.

## Declaration of Competing Interest

The authors declare that they have no known competing financial interests or personal relationships that could have appeared to influence the work reported in this paper.

## Data availability

Data will be made available on request.

## Acknowledgements

This work has been supported by the University of Rome Sapienza Projects: "Microscopic and mesoscopic organization in ionic liquid-based systems." (RG11715C7CC660BE), "Green solvents for simple and complex carbohydrates" (RM120172B2165468) and "Role of Water as an active component of neoteric solvents" (RM12117A80DF27DF). Expert support from Dr. A. Del Giudice and access to the SAXS-Lab at the University of Rome Sapienza is acknowledged. Research at ISM-CNR was supported by the project ECS00000024 "Ecosistemi dell'Innovazione"— Rome Technopole of the Italian Ministry of University and Research, public call n. 3277, PNRR— Mission 4, Component 2, Investment 1.5, financed by the European Union, Next GenerationEU.

## Appendix A. Supplementary data

Supplementary data to this article can be found online at https://doi.org/10.1016/j.molliq.2023.122120.

## References

[1] A.P. Abbott, G. Capper, D.L. Davies, R.K. Rasheed, V. Tambyrajah, Novel solvent properties of choline chloride/urea mixtures., Chem. Commun. (Camb). (2003) 70–71. b210714g.
[2] Y.H. Choi, J. van Spronsen, Y. Dai, M. Verberne, F. Hollmann, I.W.C.E. Arends, G. J. Witkamp, R. Verpoorte, Are natural deep eutectic solvents the missing link in understanding cellular metabolism and physiology? Plant Physiol. 156 (2011) 1701–1705, https://doi.org/10.1104/pp.111.178426.
[3] Y. Dai, J. van Spronsen, G.J. Witkamp, R. Verpoorte, Y.H. Choi, Natural deep eutectic solvents as new potential media for green technology, Anal. Chim. Acta. 766 (2013) 61–68, https://doi.org/10.1016/j.aca.2012.12.019.
[4] A. Paiva, R. Craveiro, I. Aroso, M. Martins, R.L. Reis, A.R.C. Duarte, Natural Deep Eutectic Solvents – Solvents for the 21st Century, ACS Sustain. Chem. Eng. 2 (2014) 1063–1071, https://doi.org/10.1021/sc500096j.
[5] Y. Liu, J.B. Friesen, J.B. McAlpine, D.C. Lankin, S.N. Chen, G.F. Pauli, Natural Deep Eutectic Solvents: Properties, Applications, and Perspectives, J. Nat. Prod. 81 (2018) 679–690, https://doi.org/10.1021/acs.jnatprod.7b00945.
[6] D.J.G.P. Van Osch, C.H.J.T. Dietz, J. Van Spronsen, M.C. Kroon, F. Gallucci, M. Van Sint Annaland, R. Tuinier, A Search for Natural Hydrophobic Deep Eutectic Solvents Based on Natural Components, ACS Sustain. Chem. Eng. 7 (2019) 2933–2942, https://doi.org/10.1021/acssuschemeng.8b03520.
[7] Y. Dai, J. Van Spronsen, G.J. Witkamp, R. Verpoorte, Y.H. Choi, Ionic liquids and deep eutectic solvents in natural products research: Mixtures of solids as extraction solvents, J. Nat. Prod. 76 (2013) 2162–2173, https://doi.org/10.1021/np400051w.
[8] R. Craveiro, I. Aroso, V. Flammia, T. Carvalho, M.T. Viciosa, M. Dionísio, S. Barreiros, R.L. Reis, A.R.C. Duarte, A. Paiva, Properties and thermal behavior of natural deep eutectic solvents, J. Mol. Liq. 215 (2016) 534–540, https://doi.org/10.1016/j.molliq.2016.01.038.
[9] E.L. Smith, A.P. Abbott, K.S. Ryder, Deep Eutectic Solvents (DESs) and Their Applications, Chem. Rev. 114 (2014) 11060–11082, https://doi.org/10.1021/cr300162p.
[10] C. D'Agostino, R.C. Harris, A.P. Abbott, L.F. Gladden, M.D. Mantle, Molecular motion and ion diffusion in choline chloride based deep eutectic solvents studied by 1H pulsed field gradient NMR spectroscopy, Phys. Chem. Chem. Phys. 13 (2011) 21383, https://doi.org/10.1039/c1cp22554e.
[11] O.S. Hammond, D.T. Bowron, K.J. Edler, Liquid structure of the choline chloride-urea deep eutectic solvent (reline) from neutron diffraction and atomistic modelling, Green Chem. 18 (2016) 2736–2744, https://doi.org/10.1039/C5GC02914G.
[12] M. Gilmore, L.M. Moura, A.H. Turner, M. Swadźba-Kwaśny, S.K. Callear, J. A. McCune, O.A. Scherman, J.D. Holbrey, A comparison of choline:urea and choline:oxalic acid deep eutectic solvents at 338 K, J. Chem. Phys. 148 (2018), 193823, https://doi.org/10.1063/1.5010246.
[13] M. Gilmore, M. Swadzba-Kwasny, J.D. Holbrey, Thermal Properties of Choline Chloride/Urea System Studied under Moisture-Free Atmosphere, J. Chem. Eng. Data. 64 (2019) 5248–5255, https://doi.org/10.1021/acs.jced.9b00474.
[14] A.H. Turner, J.D. Holbrey, Investigation of glycerol hydrogen-bonding networks in choline chloride/glycerol eutectic-forming liquids using neutron diffraction, Phys. Chem. Chem. Phys. 21 (2019) 21782–21789, https://doi.org/10.1039/c9cp04343h.
[15] O.S. Hammond, D.T. Bowron, A.J. Jackson, T. Arnold, A. Sanchez-Fernandez, N. Tsapatsaris, V. Garcia Sakai, K.J. Edler, Resilience of Malic Acid Natural Deep Eutectic Solvent Nanostructure to Solidification and Hydration, J. Phys. Chem. B. 121 (2017) 7473–7483, https://doi.org/10.1021/acs.jpcb.7b05454.
[16] O.S. Hammond, D.T. Bowron, K.J. Edler, The Effect of Water upon Deep Eutectic Solvent Nanostructure: An Unusual Transition from Ionic Mixture to Aqueous Solution, Angew. Chemie - Int. Ed. 56 (2017) 9782–9785, https://doi.org/10.1002/anie.201702486.
[17] S. Kaur, M. Kumari, H.K. Kashyap, Microstructure of Deep Eutectic Solvents: Current Understanding and Challenges, J. Phys. Chem. B. 124 (2020) 10601–10616, https://doi.org/10.1021/acs.jpcb.0c07934.
[18] A. Triolo, M.E. Di Pietro, A. Mele, F. Lo Celso, M. Brehm, V. Di Lisio, A. Martinelli, P. Chater, O. Russina, Liquid structure and dynamics in the choline acetate:urea 1:2 deep eutectic solvent, J. Chem. Phys. 154 (2021), 244501, https://doi.org/10.1063/5.0054048.
[19] P. Kumari, S. Shobhna, H.K. Kaur, Kashyap, Influence of Hydration on the Structure of Reline Deep Eutectic Solvent: A Molecular Dynamics Study, ACS Omega. 3 (2018) 15246–15255, https://doi.org/10.1021/acsomega.8b02447.
[20] E.O. Fetisov, D.B. Harwood, I.F.W. Kuo, S.E.E. Warrag, M.C. Kroon, C.J. Peters, J. I. Siepmann, First-Principles Molecular Dynamics Study of a Deep Eutectic Solvent: Choline Chloride/Urea and Its Mixture with Water, J. Phys. Chem. B. 122 (2018) 1245–1254, https://doi.org/10.1021/acs.jpcb.7b10422.
[21] M.E. Di Pietro, M. Tortora, C. Bottari, G. Colombo Dugoni, R.V. Pivato, B. Rossi, M. Paolantoni, A. Mele, In Competition for Water: Hydrated Choline Chloride:Urea vs Choline Acetate:Urea Deep Eutectic Solvents, ACS Sustain. Chem. Eng (2021), https://doi.org/10.1021/acssuschemeng.1c03811.
[22] M. Busato, V. Di Lisio, A. Del Giudice, P. Tomai, V. Migliorati, L. Galantini, A. Gentili, A. Martinelli, P. D'Angelo, Transition from molecular- to nano-scale segregation in a deep eutectic solvent - water mixture, J. Mol. Liq. 331 (2021), 115747, https://doi.org/10.1016/j.molliq.2021.115747.
[23] M. Busato, A. Tofoni, G. Mannucci, F. Tavani, A. Del Giudice, A. Colella, M. Giustini, P. D'angelo, On the Role of Water in the Formation of a Deep Eutectic Solvent Based on NiCl2·6H2O and Urea, Inorg. Chem. 61 (2022) 8843–8853, https://doi.org/10.1021/acs.inorgchem.2c00864.

[24] H. Zhang, M.L. Ferrer, R.J. Jiménez-Riobóo, F. del Monte, M.C. Gutiérrez, Tools for extending the dilution range of the "solvent-in-DES" regime, J. Mol. Liq. 329 (2021), https://doi.org/10.1016/j.molliq.2021.115573.
[25] O.S. Hammond, D.T. Bowron, A.J. Jackson, T. Arnold, A. Sanchez-fernandez, N. Tsapatsaris, V.G. Sakai, K.J. Edler, Resilience of Malic Acid Natural Deep Eutectic Solvent Nanostructure to Solidi fi cation and Hydration, (2017). 10.1021/acs.jpcb.7b05454.
[26] H. Monteiro, A. Paiva, A.R.C. Duarte, N. Galamba, On the not so anomalous water-induced structural transformations of choline chloride-urea (reline) deep eutectic system, Phys. Chem. Chem. Phys. 25 (2022) 439–454, https://doi.org/10.1039/d2cp04139a.
[27] H. Zhang, M.L. Ferrer, M.J. Roldán-Ruiz, R.J. Jiménez-Riobóo, M.C. Gutiérrez, F. Del Monte, Brillouin Spectroscopy as a Suitable Technique for the Determination of the Eutectic Composition in Mixtures of Choline Chloride and Water, J. Phys. Chem. B 124 (2020) 4002–4009, https://doi.org/10.1021/acs.jpcb.0c01919.
[28] M. Tiecco, A. Grillo, E. Mosconi, W. Kaiser, D. Giacco, R. Germani, T. Del Giacco, R. Germani, D. Giacco, R. Germani, Advances in the development of novel green liquids: thymol/water, thymol/urea and thymol/phenylacetic acid as innovative hydrophobic natural deep eutectic solvents, J. Mol. Liq. 364 (2022), 120043, https://doi.org/10.1016/j.molliq.2022.120043.
[29] A. Triolo, F. Lo Celso, O. Russina, Liquid structure of a water-based, hydrophobic and natural deep eutectic solvent: The case of thymol-water. A Molecular Dynamics study, J. Mol. Liq. 372 (2023), 121151, https://doi.org/10.1016/j.molliq.2022.121151.
[30] K.M. Harmon, G.F. Avci, Hydrogen bonding. Part 17. IR and NMR study of the lower hydrates of choline chloride, J. Mol. Struct. 118 (1984) 267–275, https://doi.org/10.1016/0022-2860(84)87223-3.
[31] E.J. Nilsson, V. Alfredsson, D.T. Bowron, K.J. Edler, A neutron scattering and modelling study of aqueous solutions of tetramethylammonium and tetrapropylammonium bromide, Phys. Chem. Chem. Phys. 18 (2016) 11193–11201, https://doi.org/10.1039/C6CP01389A.
[32] T.I. Morrow, E.J. Maginn, Density, local composition and diffusivity of aqueous choline chloride solutions: a molecular dynamics study, Fluid Phase Equilib. 217 (2004) 97–104, https://doi.org/10.1016/j.fluid.2003.08.020.
[33] S. Shaukat, M.V. Fedotova, S.E. Kruchinin, M. Bešter-Rogač, Č. Podlipnik, R. Buchner, Hydration and ion association of aqueous choline chloride and chlorocholine chloride, Phys. Chem. Chem. Phys. 21 (2019) 10970–10980, https://doi.org/10.1039/c9cp01016e.
[34] S.M. Vilas-Boas, D.O. Abranches, E.A. Crespo, O. Ferreira, J.A.P. Coutinho, S. P. Pinho, Experimental solubility and density studies on aqueous solutions of quaternary ammonium halides, and thermodynamic modelling for melting enthalpy estimations, J. Mol. Liq. 300 (2020), https://doi.org/10.1016/j.molliq.2019.112281.
[35] A. Triolo, F. Lo Celso, M. Brehm, V. Di Lisio, O. Russina, Liquid structure of a choline chloride-water natural deep eutectic solvent: A molecular dynamics characterization, J. Mol. Liq. 331 (2021), 115750, https://doi.org/10.1016/j.molliq.2021.115750.
[36] A.I.M.C. Lobo Ferreira, S.M. Vilas-Boas, R.M.A.A. Silva, M.A.R.R. Martins, D. O. Abranches, P.C.R.R. Soares-Santos, F.A. Almeida Paz, O. Ferreira, S.P. Pinho, L. M.N.B.F. Santos, J.A.P.P. Coutinho, Extensive characterization of choline chloride and its solid–liquid equilibrium with water, Phys. Chem. Chem. Phys. 24 (2022) 14886–14897, https://doi.org/10.1039/D2CP00377E.
[37] M.S. Rahman, D.E. Raynie, Thermal behavior, solvatochromic parameters, and metal halide solvation of the novel water-based deep eutectic solvents, J. Mol. Liq. 324 (2021), 114779, https://doi.org/10.1016/j.molliq.2020.114779.
[38] M. Sajjadur Rahman, J. Kyerematen, M. Saha, S. Asare, N. Uddin, M.A. Halim, D. E. Raynie, Evaluation of the experimental and computed properties of choline chloride-water formulated deep eutectic solvents, J. Mol. Liq. 350 (2022), 118520, https://doi.org/10.1016/j.molliq.2022.118520.
[39] D. Hirpara, B. Patel, V. Chavda, S. Kumar, Micellization of conventional and gemini surfactants in aquoline: A case of exclusively water based deep eutectic solvent, J. Mol. Liq. 362 (2022), 119672, https://doi.org/10.1016/j.molliq.2022.119672.
[40] Q. Abbas, P. Nürnberg, R. Ricco, F. Carraro, B. Gollas, M. Schönhoff, Less Water, Naked Choline, and Solid Iodine for Superior Ecofriendly Hybrid Energy Storage, Adv. Energy Sustain. Res. 2 (2021) 2100115, https://doi.org/10.1002/aesr.202100115.
[41] E.P. Grishina, N.O. Kudryakova, Conductivity and electrochemical stability of concentrated aqueous choline chloride solutions, Russ. J. Phys. Chem. A 91 (2017) 2024–2028, https://doi.org/10.1134/S0036024417100144.
[42] S. Shaukat, R. Buchner, Densities, viscosities [from (278.15 to 318.15) K], and electrical conductivities (at 298.15 K) of aqueous solutions of choline chloride and chloro-choline chloride, J. Chem. Eng. Data 56 (2011) 4944–4949, https://doi.org/10.1021/je200856f.
[43] K. Chai, X. Lu, Y. Zhou, H. Liu, G. Wang, Z. Jing, F. Zhu, L. Han, Hydrogen bonds in aqueous choline chloride solutions by DFT calculations and X-ray scattering, J. Mol. Liq. 362 (2022), 119742, https://doi.org/10.1016/j.molliq.2022.119742.
[44] G. Lupidi, A. Palmieri, M. Petrini, Sustainable and fast synthesis of functionalized quinoxalines promoted by natural deep eutectic solvents (NADESs), Green Chem. (2022) 3629–3633, https://doi.org/10.1039/d2gc00664b.
[45] S. Sarkar, A. Maity, R. Chakrabarti, In Silico Elucidation of Molecular Picture of Water-Choline Chloride Mixture, J. Phys. Chem. B. 125 (2021) 13212–13228, https://doi.org/10.1021/acs.jpcb.1c06636.
[46] P. Nanavare, A.R. Choudhury, S. Sarkar, A. Maity, R. Chakrabarti, Structure and Orientation of Water and Choline Chloride Molecules around a Methane Hydrophobe: A Computer Simulation Study, ChemPhysChem. 23 (2022) e202200446.
[47] R. Caminiti, V.R. Albertini, The kinetics of phase transitions observed by energy-dispersive x-ray diffraction, Int. Rev. Phys. Chem. 18 (1999) 263–299, https://doi.org/10.1080/014423599229965.
[48] M. Macchiagodena, F. Ramondo, A. Triolo, L. Gontrani, R. Caminiti, Liquid Structure of 1-Ethyl-3-methylimidazolium Alkyl Sulfates by X-ray Scattering and Molecular Dynamics, J. Phys. Chem. B 116 (2012) 13448–13458, https://doi.org/10.1021/jp306982e.
[49] L. Fernandez, L.P. Silva, M.A.R. Martins, O. Ferreira, J. Ortega, S.P. Pinho, J.A. P. Coutinho, Indirect assessment of the fusion properties of choline chloride from solid-liquid equilibria data, Fluid Phase Equilib. 448 (2017) 9–14, https://doi.org/10.1016/j.fluid.2017.03.015.
[50] N.S. Osborne, Heat of fusion of ice. A revision, J. Res. Natl. Bur. Stand. (1934). 23 (1939) 643. 10.6028/jres.023.043.
[51] M.A.R. Martins, S.P. Pinho, J.A.P. Coutinho, Insights into the Nature of Eutectic and Deep Eutectic Mixtures, J. Solution Chem. 48 (2019) 962–982, https://doi.org/10.1007/s10953-018-0793-1.
[52] Y. Xie, H. Dong, S. Zhang, X. Lu, X. Ji, Effect of Water on the Density, Viscosity, and CO 2 Solubility in Choline Chloride/Urea, J. Chem. Eng. Data 59 (2014) 3344–3352, https://doi.org/10.1021/je500320c.
[53] A.R. Harifi-Mood, R. Buchner, Density, viscosity, and conductivity of choline chloride + ethylene glycol as a deep eutectic solvent and its binary mixtures with dimethyl sulfoxide, J. Mol. Liq. 225 (2017) 689–695, https://doi.org/10.1016/j.molliq.2016.10.115.
[54] R.B. Leron, M.H. Li, High-pressure density measurements for choline chloride: Urea deep eutectic solvent and its aqueous mixtures at T = (298.15 to 323.15) K and up to 50 MPa, J. Chem. Thermodyn. 54 (2012) 293–301, https://doi.org/10.1016/j.jct.2012.05.008.
[55] A. Yadav, S. Pandey, Densities and viscosities of (choline chloride + urea) deep eutectic solvent and its aqueous mixtures in the temperature range 293.15 K to 363.15 K, J. Chem. Eng. Data. 59 (2014) 2221–2229, https://doi.org/10.1021/je5001796.
[56] V. Agieienko, R. Buchner, Densities, Viscosities, and Electrical Conductivities of Pure Anhydrous Reline and Its Mixtures with Water in the Temperature Range (293.15 to 338.15) K, J. Chem. Eng. Data. 64 (2019) 4763–4774. 10.1021/acs.jced.9b00145.
[57] D. Lapeña, F. Bergua, L. Lomba, B. Giner, C. Lafuente, A comprehensive study of the thermophysical properties of reline and hydrated reline, J. Mol. Liq. 303 (2020), 112679, https://doi.org/10.1016/j.molliq.2020.112679.
[58] C. Florindo, F.S. Oliveira, L.P.N. Rebelo, A.M. Fernandes, I.M. Marrucho, Insights into the synthesis and properties of deep eutectic solvents based on cholinium chloride and carboxylic acids, ACS Sustain. Chem. Eng. 2 (2014) 2416–2425, https://doi.org/10.1021/sc500439w.
[59] C. Andreani, C. Corsaro, D. Mallamace, G. Romanelli, R. Senesi, F. Mallamace, The onset of the tetrabonded structure in liquid water, Sci. China Physics, Mech. Astron. 62 (2019), 107008, https://doi.org/10.1007/s11433-018-9408-2.
[60] H. Jin, B. O'Hare, J. Dong, S. Arzhantsev, G.A. Baker, J.F. Wishart, A.J. Benesi, M. Maroncelli, Physical properties of ionic liquids consisting of the 1-butyl-3-methylimidazolium cation with various anions and the bis (trifluoromethylsulfonyl)imide anion with various cations, J. Phys. Chem. B. 112 (2008) 81–92, https://doi.org/10.1021/jp076462h.
[61] W. Xu, E.I. Cooper, C.A. Angell, Ionic liquids: Ion mobilities, glass temperatures, and fragilities, J. Phys. Chem. B. 107 (2003) 6170–6178, https://doi.org/10.1021/jp0275894.
[62] Y. Wang, W. Chen, Q. Zhao, G. Jin, Z. Xue, Y. Wang, T. Mu, Ionicity of deep eutectic solvents by Walden plot and pulsed field gradient nuclear magnetic resonance (PFG-NMR), Phys. Chem. Chem. Phys. 22 (2020) 25760–25768, https://doi.org/10.1039/d0cp01431a.
[63] M. McLin, C.A. Angell, Contrasting Conductance/Viscosity Relations in Liquid States of Vitreous and Polymer "Solid" Electrolytes, J. Phys. Chem. 92 (1988) 2083–2086, https://doi.org/10.1021/j100319a002.
[64] L. Bahadori, M.H. Chakrabarti, F.S. Mjalli, I.M. Alnashef, N.S.A. Manan, M. A. Hashim, Physicochemical properties of ammonium-based deep eutectic solvents and their electrochemical evaluation using organometallic reference redox systems, Electrochim. Acta. 113 (2013) 205–211, https://doi.org/10.1016/j.electacta.2013.09.102.
[65] D.Z. Troter, Z.B. Todorović, D.R. Đokić-Stojanović, B.S. Đordević, V.M. Todorović, S.S. Konstantinović, V.B. Veljković, The physicochemical and thermodynamic properties of the choline chloride-based deep eutectic solvents, J. Serbian Chem. Soc. 82 (2017) 1039–1052, https://doi.org/10.2298/JSC170225065T.
[66] R.B. Leron, A.N. Soriano, M.H. Li, Densities and refractive indices of the deep eutectic solvents (choline chloride+ethylene glycol or glycerol) and their aqueous mixtures at the temperature ranging from 298.15 to 333.15K, J. Taiwan Inst. Chem. Eng. 43 (2012) 551–557, https://doi.org/10.1016/j.jtice.2012.01.007.
[67] K.M. Harmon, A.C. Akin, G.F. Avci, L.S. Nowos, M.B. Tierney, Hydrogen bonding. Part 33. NMR study of the hydration of choline and acetylcholine halides, J. Mol. Struct. 244 (1991) 223–236. 10.1016/0022-2860(91)80158-Z.
[68] C. D'Agostino, L.F. Gladden, M.D. Mantle, A.P. Abbott, E.I. Ahmed, A.Y.M. Al-Murshedi, R.C. Harris, Molecular and ionic diffusion in aqueous-deep eutectic solvent mixtures: Probing inter-molecular interactions using PFG NMR, Phys. Chem. Chem. Phys. 17 (2015) 15297–15304, https://doi.org/10.1039/c5cp01493j.
[69] M.J. Roldán-Ruiz, R.J. Jiménez-Riobóo, M.C. Gutiérrez, M.L. Ferrer, F. del Monte, Brillouin and NMR spectroscopic studies of aqueous dilutions of malicine: Determining the dilution range for transition from a "water-in-DES" system to a "DES-in-water" one, J. Mol. Liq. 284 (2019) 175–181, https://doi.org/10.1016/j.molliq.2019.03.133.

[70] E. Posada, N. López-Salas, R.J. Jiménez Riobóo, M.L. Ferrer, M.C. Gutiérrez, F. Del Monte, Reline aqueous solutions behaving as liquid mixtures of H-bonded co-solvents: Microphase segregation and formation of co-continuous structures as indicated by Brillouin and 1H NMR spectroscopies, Phys. Chem. Chem. Phys. 19 (2017) 17103–17110, https://doi.org/10.1039/c7cp02180a.
[71] E. Veroutis, S. Merz, R.A. Eichel, J. Granwehr, Intra- and inter-molecular interactions in choline-based ionic liquids studied by 1D and 2D NMR, J. Mol. Liq. 322 (2021), 114934, https://doi.org/10.1016/j.molliq.2020.114934.
[72] P.G. Gordon, D.H. Brouwer, J.A. Ripmeester, Probing the Local Structure of Pure Ionic Liquid Salts with Solid- and Liquid-State NMR, ChemPhysChem. 11 (2010) 260–268, https://doi.org/10.1002/cphc.200900624.
[73] D.L. Bryce, M. Gee, R.E. Wasylishen, High-field chlorine NMR spectroscopy of solid organic hydrochloride salts: A sensitive probe of hydrogen bonding environment, J. Phys. Chem. A. 105 (2001) 10413–10421, https://doi.org/10.1021/jp011962a.
[74] M.E. Di Pietro, O. Hammond, A. Van Den Bruinhorst, A. Mannu, A. Padua, A. Mele, M. Costa Gomes, Connecting chloride solvation with hydration in deep eutectic systems, Phys. Chem. Chem. Phys. 23 (2021) 107–111, https://doi.org/10.1039/d0cp05843b.
[75] C.D. Agostino, L.F. Gladden, M.D. Mantle, A.P. Abbott, I. Ahmed, A.Y.M. Al-murshedi, R.C. Harris, Molecular and ionic diffusion in aqueous – deep eutectic solvent mixtures : probing inter-molecular interactions using PFG NMR, Phys. Chem. Chem. Phys. 17 (2015) 15297–15304, https://doi.org/10.1039/C5CP01493J.